# Measurement of the backward-to-90° neutron-proton elastic cross section ratio between 40 and 75 MeV

A. Bol, C. Dupont, P. Leleux, P. Lipnik, P. Macq, and A. Ninane
*Institut de Physique, Université Catholique de Louvain,*
*B-1348 Louvain-la-Neuve, Belgium*
(Received 25 February 1985)

The ratio of the 166° c.m. to 90° c.m. and of the 178.5° c.m. to 90° c.m. differential cross section for neutron-proton scattering has been measured between 40 and 75 MeV. The trend of our data is slightly higher than the present phase-shift analysis.

The backward-to-90° ratio of the neutron-proton differential cross section is a good test of the potentials aiming at the description of the two-nucleon system. In fact, in our energy range, the 90° cross section should be fairly well determined from the total cross section, whereas the backward angle cross section checks the two-nucleon wave function in the medium range in view of the momentum transfer involved. In the 40–80 MeV domain the Paris potential, one of the best candidates, is in disagreement with the phase-shift analysis at backward angle. However, most of the data have a large error bar, as it is shown in Fig. 1 for the 166° to 90° ratio prior to our work. Data points are from Harwell[1] and Davis.[2] The solid curve is a recent global phase-shift analysis,[3] while the dashed curve is the Paris potential calculation.[4] The goal of the present work was to achieve a precision better than the discrepancy between the phase-shift analysis and the Paris potential calculation. This paper reports on the measurement of the 166°/90° and of the 178.5°/90° ratio between 40–75 MeV.

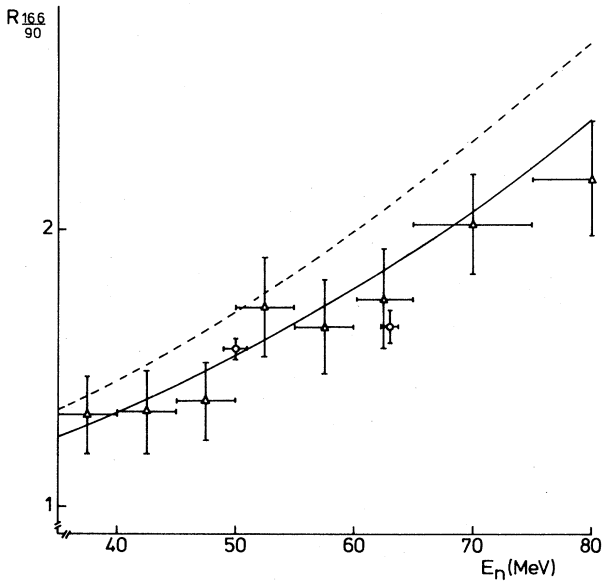


FIG. 1. Experimental values of the ratio of the 166° to 90° n-p elastic cross section ($R_{166/90}$), prior to this work. Data are from Harwell (triangles, Ref. 1) and Davis (open dots, Ref. 2). The solid curve is the phase-shift analysis, the dashed curve is the Paris potential calculation.

The neutron beam has been already described at length.[5] In brief, a 5 $\mu$A proton beam from the Louvain isochronous cyclotron bombards a 6 mm or 1 cm thick Li target. Behind the target, an electromagnet bends the protons downstairs by a few cm into a carbon Faraday cup. With respect to the original setup,[5] this is an improvement in the sense that the carbon beam stop is now out of sight of the neutron collimator entrance (7 mm diameter). Neutrons at 0° are selected by a laser-aligned conical iron collimator made of three separate parts: a first one immediately behind the Faraday cup, 2 m long, with a final diameter of 11.2 mm; a second one, 40 cm long at 4.1 m from the Li target with a final diameter of 14.4 mm; and finally a third part, 80 cm long, starting at 5.8 m from the lithium with a final diameter of 20 mm. At 6.7 m from the lithium, neutrons interact with a 5-mm-thick liquid hydrogen target, limited by 6-$\mu$m-thick aluminized Mylar windows. The charged particles contaminating the neutron beam are vetoed by a 0.1-mm-thick plastic scintillator in front of the hydrogen target. Immediately behind the target, another 0.1-mm-thick plastic scintillator (START) triggers on charged particles from the target. Three plastic scintillators (STOP) are used to detect and select elastically scattered protons: a first one, 3 cm diameter and 1 mm thick, at 45° lab, a second one, 3 cm diameter and 1 mm thick, at 7° lab, and a third one, annular with an internal (external) diameter of 35(45) mm, at a mean angle of 0.8° lab. The first two are at 1 m from the target, the third one at 1.5 m. The whole setup is kept under vacuum (see Fig. 2).

The time-of-flight (TOF) between the START and each of the three STOP scintillators, and the TOF between the

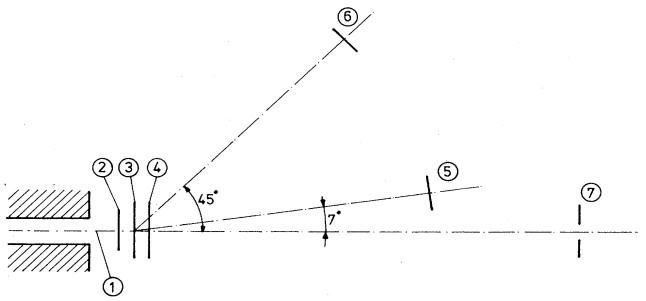


FIG. 2. Sketch of the experimental setup: 1, collimated neutron beam; 2, veto detector; 3, liquid hydrogen target; 4, start detector; 5, 6, and 7, stop detectors. The distance from 3–5 or 6 is 1 m, from 3–7 is 1.5 m.

 

START and a capacitive beam pick-off (BPO) upstream of the Li target, are recorded for each event, as well as the amplitude signal from each detector. Events are stored on magnetic tape via a CAMAC interface and a computer. Runs normalized to the Faraday cup integrated current are alternated for a hydrogen and an empty target. The cyclotron burst duration was optimized at each energy using a movable slit near the center by minimizing the width of the $\gamma$-ray peak appearing in the TOF spectrum between the BPO and a lucite block coupled to a photomultiplier in the neutron beam at 9 m from the Li target. The full width at half-maximum ranged between 1 and 1.5 nsec depending on the energy.

Data analysis proceeds as follows: Monoenergetic neutrons from the $^7$Li(p,n)$^7$Be reaction are first selected from the START-BPO TOF (Fig. 3) (this spectrum is measured modulo one RF period, low energy neutrons from the preceding burst are thus also retained in this selection). Three START-STOP spectra are reconstructed; each one is dominated by a proton peak corresponding to n-p scattering due to high-energy neutrons; low energy protons from the above mentioned contamination are easily separated by the TOF (Fig. 4). The empty target contribution is about 3% of the signal at each energy. The ratio of the solid angles of the STOP detectors was measured with a 1% precision, using an $\alpha$ source located at the hydrogen target position.

At 65 MeV, an independent measurement was performed the following way: The START and the VETO detectors were pulled out; at 7° lab, were set two 1-mm-thick scintillators, the first (second) one of 3(4) cm diameter. A copper absorber was put between the two scintillators. The same arrangement was done at 45° lab. At both angles, the copper thickness was calculated in such a way that requesting a coincidence between both scintillators should select protons elastically scattered by neutrons from the high-energy peak. Only two spectra were recorded, namely, the TOF between the 7° or 45° coincidence and the BPO. Each one contained only a narrow peak which was integrated. The empty target contribution was subtracted. In fact this was really a scaler-type experiment as opposed to the multiparameter data taking of the main part of this work. Both

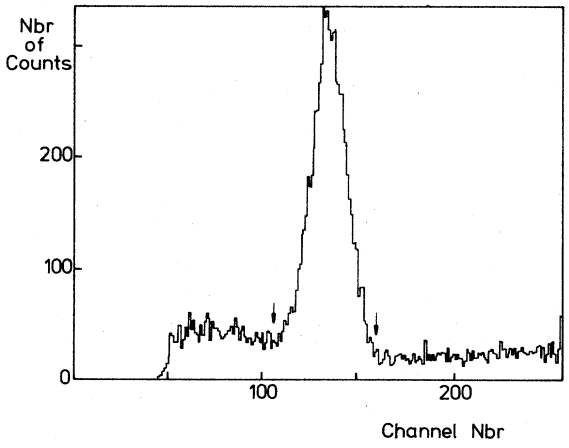


FIG. 3. Typical START-BPO TOF spectrum showing the high-energy peak from the Li target. The software window limits are indicated by arrows. The horizontal time scale is 0.1 nsec/channel.

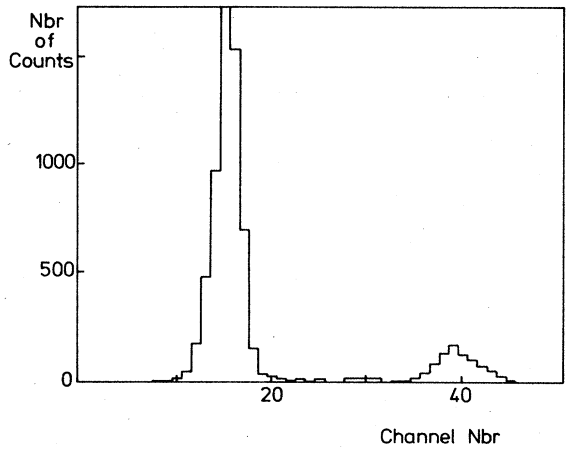


FIG. 4. Typical START-STOP TOF spectrum for the 7° detector, for the hydrogen target. The horizontal time scale is 0.4 nsec/channel.

were in perfect agreement.

The measured values of the ratios

$$\frac{d\sigma}{d\Omega}(166°) \Big/ \frac{d\sigma}{d\Omega}(90°)$$

and

$$\frac{d\sigma}{d\Omega}(178.5°) \Big/ \frac{d\sigma}{d\Omega}(90°)$$

from this work are plotted in Figs. 5 and 6, whereas numerical values can be found in Table I. At 50 MeV, the precise (166°/90°) data point from Davis[1] is in perfect agreement with this work. For the (178.5°/90°) ratio no other data exist. On both figures are also shown the phase-shift analysis[3] and the Paris potential[4] calculation. The trend of our data is slightly higher than the previous data, which is apparent from a comparison with the phase-shift analysis. Finally it should be mentioned that in a first version of this experiment the use of a much shorter neutron flight path (2 m)

TABLE I. Experimental values for the ratio of the 166° to 90° differential cross section ($R_{166/90}$) and of the 178.5° to 90° cross section ($R_{178/90}$), from this work. The uncertainty is the statistical error. The quoted neutron energy was obtained by subtracting from the incident proton energy, the proton energy loss in half the lithium thickness and the $Q$ value of the $^7$Li(p,n) reaction. The uncertainty on the neutron energy is due to the Li thickness.

| $E_n$ (MeV) | $R_{166/90}$ | $R_{178/90}$ |
|---|---|---|
| 40. ±1.6 | 1.39 ±0.03 | 1.49 ±0.03 |
| 45. ±1.5 | 1.47 ±0.03 | 1.57 ±0.03 |
| 50. ±1.4 | 1.59 ±0.03 | 1.70 ±0.04 |
| 55.1 ±1.3 | 1.75 ±0.04 | 1.82 ±0.05 |
| 61. ±1.2 | 1.87 ±0.04 | · · · |
| 62.2 ±1. | 1.90 ±0.05 | 1.98 ±0.06 |
| 65. ±1. | 2.00 ±0.04 | 2.14 ±0.10 |
| 70. ±1. | 2.10 ±0.05 | 2.33 ±0.06 |
| 76.2 ±2. | 2.22 ±0.07 | · · · |

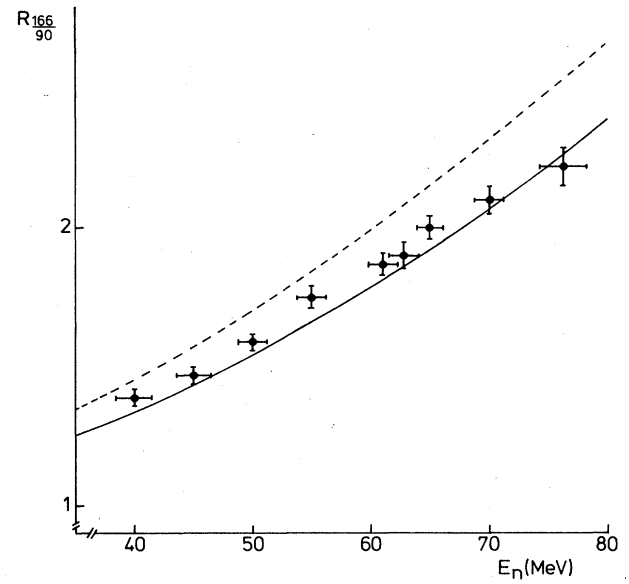


FIG. 5. $R_{166/90}$ from this work. The meaning of the curves is the same as in Fig. 1.

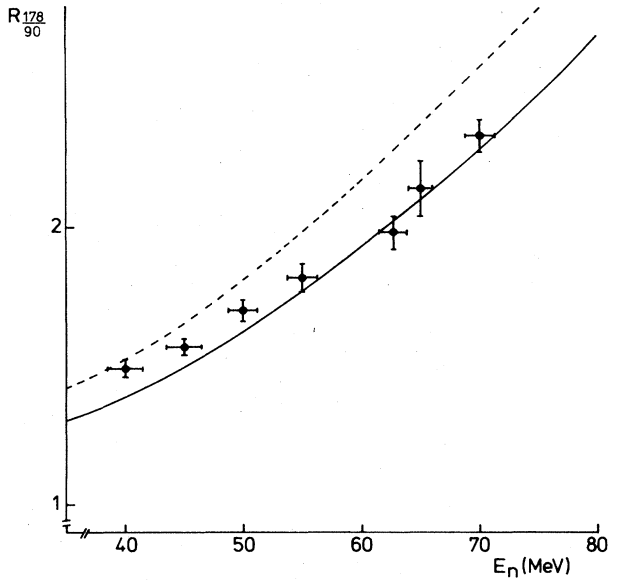


FIG. 6. $R_{178/90}$ from this work. The meaning of the curves is as in Fig. 1.

and the absence of a clearing magnet between the Li target and the carbon beam stopper had caused an important background of gamma rays and low energy neutrons, not only in the beam but also at small lab angles. This had led us to erroneously overestimate the 170°–90° cross section ratio.[6]

We wish to thank the cyclotron staff. This research was supported by the Institut Interuniversitaire des Sciences Nucléaires, Belgium. Two of us (P.L. and A.N.) thank the National Fund for Scientific Research, Belgium, for financial support.

[1]J. P. Scanlon *et al.*, Nucl. Phys. **41**, 401 (1963).
[2]T. C. Montgomery *et al.*, Phys. Rev. C **16**, 499 (1977); N. S. P. King *et al.*, *ibid.* **21**, 1185 (1980).
[3]R. A. Arndt and L. D. Roper, NN interactive program (solution WI83).
[4]R. Vinh Mau (private communication).
[5]A. Bol *et al.*, Nucl. Instrum. Methods **214**, 169 (1983).
[6]A. Bol *et al.*, in *Few Body Problems in Physics,* Proceedings of the Tenth International IUPAP Conference, Karlsruhe, 1983, edited by B. Zeitnitz (North-Holland, Amsterdam, 1984), Vol. II, p. 23.